HHS Public Access

Author manuscript

Brain Res. Author manuscript; available in PMC 2017 April 01.

Published in final edited form as:

Brain Res. 2016 April 1; 1636: 62–73. doi:10.1016/j.brainres.2016.01.045.

Light and electron microscopic analysis of enkephalin-like immunoreactivity in the basolateral amygdala, including evidence for convergence of enkephalin-containing axon terminals and norepinephrine transporter-containing axon terminals onto common targets

Jingyi Zhang[1] and **Alexander J. McDonald**[*]

Department of Pharmacology, Physiology and Neuroscience, University of South Carolina School of Medicine, Columbia, SC 29208

Abstract

Modulatory interactions of opioids and norepinephrine (NE) in the anterior subdivision of the basolateral nucleus of the amygdala (BLa) are critical for the consolidation of memories of emotionally arousing experiences. Although there have been several studies of the noradrenergic system in the amygdalar basolateral nuclear complex (BLC), little is known about the chemical neuroanatomy of opioid systems in this region. To address this knowledge gap the present study first examined the distribution of met-enkephalin-like immunoreactivity (ENK-ir) in the BLC at the light microscopic level, and then utilized dual-labeling immunocytochemistry combined with electron microscopy to investigate the extent of convergence of NE and ENK terminals onto common structures in the BLa. Antibodies to ENK and the norepinephrine transporter (NET) were used in these studies. Light microscopic examination revealed that a subpopulation of small nonpyramidal neurons expressed ENK-ir in all nuclei of the BLC. In addition, the somata of some pyramidal cells exhibited light to moderate ENK-ir. ENK+ axon terminals were also observed. Ultrastructural analysis confined to the BLa revealed that most ENK+ axon terminals formed asymmetrical synapses that mainly contacted spines and shafts of thin dendrites. ENK+ terminals forming symmetrical synapses mainly contacted dendritic shafts. Approximately 20% of NET+ terminals contacted a structure that was also contacted by an ENK+ terminal and 6% of NET+ terminals contacted an ENK+ terminal. These findings suggest that ENK and NE terminals in the BLa may interact by targeting common dendrites and by direct interactions between the two types of terminals.

[*]**Correspondence to**: Alexander J. McDonald, Telephone: 803-216-3511 Fax: 803-216-3524, alexander.mcdonald@uscmed.sc.edu.

[1]Present address: Department of Pharmacology & Physiology, Drexel University College of Medicine, Philadelphia, PA 19102

Conflict of interest

The authors indicate no potential conflicts of interest.

Keywords

Opioids; Immunohistochemistry; Nonpyramidal neurons; Ultrastructure; Synapse; Axon terminals

1. Introduction

Accumulating evidence indicates that norepinephrine (NE) and opioid systems in the anterior subdivision of the basolateral nucleus of the amygdala (BLa) are critical for stress adaptation and memory consolidation of emotionally arousing experiences (Introini-Collison et al., 1995; Drolet et al., 2001; McGaugh, 2004; Roozendaal et al., 2009). Stressful stimuli such as footshock induce norepinephrine release in the rat BLa (Galvez et al., 1996; Quirarte et al., 1998). Post-training drug treatment studies using adrenergic agonists and antagonists indicate that activating the NE system in the BLa enhances memory retention of inhibitory avoidance whereas inhibiting the NE system impairs memory retention (Ferry and McGaugh, 1999; McGaugh, 2004; Ferry and McGaugh, 2008).

Endogenous opioid peptides include endorphin, enkephalin and dynorphin, which are derived, respectively, from three peptide precursors: proopiomelanocortin, proenkephalin and prodynorphin (Drolet et al., 2001). These opioid peptides produce their effects via three types of G-protein coupled receptors: mu, delta and kappa. The opioid antagonist naloxone has been found to enhance memory retention of inhibitory avoidance, and this effect is reversed by mu opioid receptor (MOR) agonists (Izquierdo and Graudenz, 1980; Introini-Collison et al., 1989; Introini-Collison et al., 1995). Memory regulating effects of opioids are believed to be mediated, at least in part, through the modulation of the NE system in the BLa, since intra-amygdalar activation of MORs impairs memory by inhibiting NE release, and facilitating NE function compensates for these memory impairment effects (Introini-Collison et al., 1995; McGaugh, 2004). Enkephalin or enkephalin-like peptides are the most likely activators of MORs in the BLa, since the BLa receives an extremely sparse innervation by beta-endorphin containing axons (Gray et al., 1984), the other main opioid peptide associated with MORs, and met-enkephalin (ENK) has been shown to inhibit NE release in the BLa (Tanaka et al., 2000).

In addition to the inhibition of NE release by ENK acting presynaptically, it is also possible that there could be postsynaptic interactions of the ENK and NE systems. The major postsynaptic targets of NE inputs in the BLa are distal dendrites and spines of pyramidal projection neurons (Zhang et al., 2013). These structures are also the main components that express β-adrenergic receptors (Farb et al., 2010) and MORs (Zhang et al., 2015), which suggests that NE and ENK inputs might both synapse with these postsynaptic structures, similar to the locus ceruleus where ENK and epinephrine terminals converge on the same dendrites (Van Bockstaele et al., 1996). However, there have been no detailed light or electron microscopic studies of ENK immunoreactivity (ENK-ir) in the basolateral amygdala, nor have any previous studies examined the convergence of ENK and NE terminals onto common structures. The present study first examined the distribution of ENK-ir in the basolateral amygdala at the light microscopic level, and then utilized dual-labeling immunocytochemistry at the ultrastructural level, using antibodies to ENK and the

norepinephrine transporter (NET), to investigate the extent of convergence of NE and ENK terminals onto common structures in the BLa. In addition, the types of synapses formed by ENK-immunoreactive (ENK+) terminals, as well as their postsynaptic targets, were analyzed.

2. Results

2.1 Light microscopic observations of enkephalin-like immunoreactivity

The distribution pattern of ENK-ir in the amygdala was similar in sections stained with nickel-intensified or non-intensified diaminobenzidine (DAB), but all structures were more intensely stained with the former chromogen (Figs. 1 and 2). The most intense ENK staining in the amygdala was seen in the central nucleus, especially in its lateral and lateral capsular subdivisions (Fig. 1A, B). There were many ENK+ somata (12–13 μm in diameter) as well as dense neuropilar staining in these lateral portions of the central nucleus. Lighter ENK neuropilar staining and only a few ENK+ somata were seen in the medial subdivision of the central nucleus. The intercalated nuclei, located lateral, medial and within the basolateral nuclear complex (BLC; consisting of the lateral, basolateral, and basomedial nuclei), exhibited moderate to dense neuropilar ENK-ir (Fig. 1A, B). The intercalated nuclei also contained somata (7–8μm in diameter) that exhibited light to moderate ENK-ir.

ENK neuropilar staining in the nuclei of the BLC was relatively light compared to the central and intercalated nuclei (Fig. 1). All portions of the BLC, as well as the cortical nuclei and amygdalohippocampal area, contained small nonpyramidal neurons that exhibited moderate to strong ENK-ir (Figs.1C, D; Fig. 2A, C, Fig. 3). Their small somata were usually ovoid and 8–12 μm in diameter (Figs. 2A, C). These nonpyramidal ENK+ neurons gave off 3–4 thin aspiny primary dendrities that branched sparingly (Fig. 2A). The axons of some of these neurons were observed; they arose from the cell body and could be followed for 10–50 μm before becoming lost in the neuropil. In addition to the labeling of nonpyramidal neurons there was light ENK-ir in numerous larger neurons with pyramidal or piriform somata that obviously belonged to pyramidal neurons. The somata of pyramidal neurons in the ventral portions of the BLa, which were about 13–18 μm long and 10–12 μm wide, exhibited stronger ENK-ir than those in other portions of the BLC (Figs. 1C, D). Varicose ENK+ axons were observed in all portions of the BLC, as well as in the cortical nuclei and amygdalohippocampal area. In the BLa and posterior basolateral nucleus (BLp) most of the axonal varicosities were very small and lightly stained, but occasional larger varicosities (ca. 1 μm in diameter) with dense ENK-ir were observed (Fig. 2A). The density of axons with both small and large varicosities was much greater in the lateral nucleus than in the basolateral nuclei (Figs. 2A, B). The vast majority of both types of axons was located in the neuropil, and did not appear to contact either pyramidal or nonpyramidal ENK+ somata.

2.2 Electron microscopic observations

Particulate reaction product (generated using Vector-VIP [Very Intense Purple] as a chromogen, see Experimental Procedures) representing ENK-ir was seen in a variety of neuronal profiles including somata, dendrites, spines, axons, and axon terminals. ENK-ir in somata was sparse and confined to a few particles in the Golgi complex whereas most ENK-

ir in dendrites, spines, axons and axon terminals was diffusely distributed (Figs. 4 and 5). ENK+ terminals were round to ovoid, and most were 0.5–0.75 μm in diameter. Synaptic vesicles in most ENK+ terminals were small, clear, and round or oval. Larger dense core vesicles, which were seen in a small number of ENK+ terminals, were typically located distant to the active zone of synapses. A total of 68.4% (158/231) of ENK+ terminals were observed forming synapses with either ENK+ or unlabeled structures. Nine of these 158 ENK+ terminals formed two synapses, for a total of 167 synapses. ENK+ terminals mainly formed asymmetrical synapses (85% of synapses; 142/167) and their most frequent targets were ENK+ and ENK-negative spines (Table 1; Fig. 4B). Symmetrical synapses formed by ENK+ terminals constituted 15% of all synapses (25/167) and their most frequent targets were thin ENK+ dendritic shafts (Table 1).

At the light microscopic level the monoclonal NET antibody stained a dense plexus of varicose axons in the BLa (Fig. 2D). At the electron microscopic level NET+ profiles consisted of thin unmyelinated axons and axon terminals containing synaptic vesicles (Figs. 4 and 5). The DAB peroxidase reaction product was diffusely distributed throughout these NET + profiles, with accumulations near the plasma membrane and the outer membrane of vesicles and mitochondria. This diffuse DAB reaction product was easily distinguished from the particulate Vector-VIP reaction product of ENK-ir. NET+ terminals were round or ovoid in shape with closely packed small, round, clear synaptic vesicles, and occasional large clear vesicles or large dense core vesicles (Fig. 4A), similar to the descriptions of DBH+ profiles and NET+ profiles reported in previous studies of the basolateral amygdala (Asan, 1998; Li et al., 2001; Li et al., 2002; Farb et al., 2010; Zhang et al., 2013). NET terminals mainly formed symmetrical synapses, and they targeted both ENK+ and unlabeled structures, including dendritic shafts, spines and somata, consistent with previous studies (Li et al., 2001; Li et al., 2002; Zhang et al., 2013).

Approximately 20% (16/78) of NET+ terminals in the BLa contacted a structure that was also contacted by an ENK+ terminal (Fig. 5). The targets and types of contacts formed by converging terminals are listed in Table 2. In general, the most frequent common targets were small-caliber dendritic shafts and spines (Fig. 5; Table 2). In most instances of convergence, ENK+ terminals formed asymmetrical synapses or appositions whereas NET+ terminals formed symmetrical synapses or appositions (Table 2). In addition, NET+ and ENK+ terminals contacted each other in five cases (6.4% [5/78] of NET+ terminals) (Fig. 5B, C).

3. Discussion

This is the first investigation to study the ultrastructural localization of ENK in the BLa, as well as the possible convergence of NET+ and ENK+ axon terminals onto common structures in this nucleus. Our results demonstrate that ENK is expressed in at least two neuronal subpopulations in the BLa: pyramidal neurons and a subpopulation of small nonpyramidal neurons. Ultrastructural analysis confined to the BLa revealed that most ENK + axon terminals formed asymmetrical synapses that mainly contacted spines and shafts of thin dendrites. ENK+ terminals forming symmetrical synapses mainly contacted dendritic shafts. Approximately 20% of NET+ terminals contacted a structure that was also contacted

by an ENK+ terminal and 6% of NET+ terminals contacted an ENK+ terminal. These findings suggest that ENK and NE terminals in the BLa may interact by targeting common dendrites and by direct interactions between the two types of terminals.

3.1 Pyramidal neurons and small nonpyramidal neurons in the basolateral amygdala express ENK-ir

Although most pyramidal neurons in the basolateral amygdala at the light microscopic level exhibited little or no ENK-ir, perikarya of pyramidal neurons located in the ventral and ventromedial portions of the BLa were moderately stained. Since it is well established that BLa pyramidal neurons like cortical pyramidal neurons, use glutamate as a neurotransmitter (Sah et al., 2003; Pape and Pare, 2010), these findings are consistent with in situ hybrization studies which found that pyramidal neurons in these portions of BLa co-express mRNAs for preproenkephalin and vesicular glutamate transporter 1 (VGLUT1), a marker for glutamatergic neurons (Poulin et al., 2008). In fact, 95% of neurons in the BLa that expressed mRNA for preproenkephalin also expressed mRNA for VGLUT1 (Poulin et al., 2008). It is also of interest that preliminary studies in colchicine-injected animals in our lab have demonstrated that ENK-ir accumulates in the axon initial segments of these pyramidal neurons (personal observations of AJM), suggesting that ENK is transported to the axon terminals of these neurons. Since the great majority of spines in the BLa originate from dendritic shafts of pyramidal neurons (Muller et al., 2006), most of the ENK+ spines and spiny dendrites seen at the ultrastructural level are undoubtedly of pyramidal cell origin.

Numerous small nonpyramidal interneurons expressing ENK-ir were seen throughout the basolateral amygdala. These have been described in previous studies of the amygdala using antibodies to met-enkephalin, enkephalin-7, and leu-enkephalin (Finley et al., 1981; Khachaturian et al., 1983; Merchanthaler et al., 1986; Wilson et al., 2002). In some of these studies injections of colchicine were required for adequate visualization of these cells. In the present study they were strongly stained with nickel-intensified DAB, and more weakly stained in sections stained with non-intensified DAB, in non-colchicine-injected rats. Their distinctive morphology (i.e., small perikaryon and very thin dendrites) closely resembles that of small nonpyramidal neurons in the basolateral and lateral nuclei that co-express vasoactive intestinal peptide (VIP), the calcium binding protein calretinin (CR), and cholecystokinin (CCK) (Mascagni and McDonald, 2003). In fact, preliminary studies performed in our lab have demonstrated that ENK+ neurons constitute a subpopulation of VIP+ and CR+ nonpyramidal neurons (personal observations of AJM). Likewise, ENK+ nonpyramidal neurons in the hippocampus also express VIP and CR (Blasco-Ibáñez et al., 1998). Since these small basolateral nonpyramidal neurons, like other nonpyramidal neuronal subpopulations in the basolateral amygdala, are GABAergic (McDonald and Pearson, 1989; McDonald and Mascagni, 2001), they undoubtedly correspond to the neurons of the lateral nucleus that co-express mRNAs for preproenkephalin and glutamate decarboxylase 65 (GAD65) (Poulin et al., 2008). Although we observed small ENK+ nonpyramidal neurons in all portions of the basolateral amygdala, very few neurons co-expressing preproenkephalin and GAD65 mRNAs were observed in the basolateral nucleus by Poulin and co-workers (2008).

3.2 ENK-ir is found in axon terminals in the BLa

ENK+ axon terminals mainly formed asymmetrical synapses in the BLa (85%), but symmetrical synapses were also observed (15%). The percentage of symmetrical synapses may be underestimated since they are more difficult to detect if the plane of section is oblique to the synaptic junction. It is well established that in the BLa, as in the cortex, axons with terminals forming asymmetrical and symmetrical synapses are mainly glutamatergic and GABAergic, respectively (Smith and Pare´, 1994; McDonald et al., 2002). ENK can be co-released with glutamate or GABA in these axons when they fire at high frequencies (Wagner et al., 1990). ENK released from dense core vesicles located in axon terminals or non-synaptic intervaricose segments of axons (van den Pol, 2012) can activate mu (MOR) and delta (DOR) opioid receptors, both of which are found in very high concentrations in the BLa (Mansour et al., 1987, 1995). Although there have been no ultrastructural studies of DORs in the BLa, recent studies of MORs indicate that they are expressed in axon terminals, as well as in dendrites and spines (Glass et al., 2005; Zhang et al., 2015). Enkephalin or enkephalin-like peptides are the most likely activators of almost all MORs in the BLa, since the BLa receives an extremely sparse innervation by beta-endorphin containing axons (Gray et al., 1984), the other main opioid peptide associated with MORs. ENK released from BLa axons may reach MORs in dendrites via “wired” synaptic transmission or by diffusion in the extracellular space (“volume” or “parasynaptic” transmission) (Agnati et al., 1986). Activation of MORs in axon terminals would require volume transmission, but activation of MOR autoreceptors at synapses formed by ENK+/MOR+ terminals is also possible (see below).

One likely origin of ENK+ axons forming asymmetrical (putative glutamatergic) synapses are the local ENK+ pyramidal neurons in the BLa (see above), since these neurons have extensive local axonal arborizations (Pitkänen et al., 2003; McDonald et al., 2005). These axons would thus release the excitatory neurotransmitter glutamate as well as ENK, which would be expected to have largely inhibitory actions via activation of MORs or DORs associated with Gi protein signaling pathways (Wagner and Chavkin, 1995). Other possible origins of ENK+ axons forming asymmetrical synapses are afferents from the cerebral cortex (Hall, 1972; Smith and Paré, 1994; Brinley-Reed et al., 1995; Farb and LeDoux, 1999; Smith et al., 2000, Pinard et al., 2010) and thalamus (Carlsen and Heimer, 1988; LeDoux et al., 1991), but it is unclear whether these inputs are enkephalinergic. The main postsynaptic targets of terminals forming asymmetrical synapses, including the ENK+ terminals in the present study, are spines, the great majority of which arise from distal dendrites of BLa pyramidal neurons (Muller et al., 2006). MORs in the BLa are expressed in both axon terminals forming asymmetrical synapses as well as in spines (Zhang et al., 2015). Electrophysiological studies have shown that the ENK analog DAMGO ([D-Ala2, N-MePhe4, Gly-ol]-enkephalin), a MOR agonist, activates a voltage-dependent potassium current in dendrites, but not in the somata, of pyramidal neurons in the BLC (Faber and Sah, 2004). Since glutamatergic inputs to BLa pyramidal neurons synapse with dendrites but not somata (Muller et al., 2006), it is likely that ENK released from glutamatergic axons may activate this dendritic current in vivo. DAMGO also inhibits glutamate release onto pyramidal neurons of the BLa via presynaptic MOR activation (Yang et al., 2014). It is possible that the mechanism of action for this effect involves activation of MOR

autoreceptors in glutamatergic axon terminals by ENK released from these axons (Zhang et al., 2015). ENK released from glutamatergic terminals might also activate MORs in neighboring glutamatergic terminals synapsing with other spines via volume transmission (Drake et al., 2002).

ENK+ axon terminals in the BLa that form symmetrical (putative GABAergic or neuromodulatory) synapses mainly target ENK+ dendritic shafts, but it is not clear whether these are dendrites of pyramidal neurons, nonpyramidal interneurons, or both. These ENK+ terminals may belong to the axons of the small ENK+ BLa nonpyramidal interneurons and/or the ENK+ neurons of the intercalated nuclei observed in the present study. Both of these neuronal populations exhibit colocalization of ppENK and GAD65 mRNA (Poulin et al., 2008), and have axons that innervate neurons in the BLa (Muller et al., 2003; Marowsky et al., 2005). These axons presumably release the inhibitory neurotransmitter GABA as well as ENK, which like GABA would be expected to have largely inhibitory actions (Wagner and Chavkin, 1995). DAMGO can inhibit the release of GABA from terminals in the basolateral amygdala (Sugita and North, 1993), including GABAergic terminals that synapse with pyramidal neurons (Finnegan et al., 2005). The finding of the present study that some putative GABAergic terminals contain ENK suggests that ENK released from these same terminals may be responsible for these presynaptic effects via an MOR-mediated autoreceptor mechanism (Zhang et al., 2015). ENK/MOR mediated inhibition of GABA release should increase the excitability and firing of pyramidal neurons that are postsynaptic to these inhibitory terminals via a disinhibitory mechanism. Indeed, one of the major targets of GABAergic VIP+ interneurons, some of which express ENK (see above), are presumptive pyramidal cells (Muller et al., 2003). In addition, it is possible that ENK released from interneuronal axons could inhibit pyramidal cell dendrites by activating voltage-dependent potassium currents (Faber and Sah, 2004).

In addition to innervating BLa pyramidal neurons, VIP+ interneurons in the BLa innervate dendrites of other GABAergic interneurons that express calbindin (Muller et al., 2003). This finding suggests that ENK released from the axons of ENK+/VIP+ neurons could inhibit the dendrites of one or both of the two main types of calbindin-containing GABAergic interneurons, parvalbumin (PV) and/or somatostatin (SOM) expressing neurons, if these interneurons express MORs or DORs (McDonald and Mascagni, 2001, 2002). Indeed, there is evidence that dendrites of BLa interneurons, including PV+ neurons, express MORs (Zhang et al., 2015). Since PV+ and SOM+ interneurons inhibit pyramidal cells (Muller et al., 2006, 2007; Woodruff and Sah, 2007), ENK might have a disinhibitory effect on BLa pyramidal cells via a disynaptic mechanism. Interestingly, the sole targets of ENK+/VIP+ and ENK+/CR+ interneurons in the hippocampus are other interneurons (Blasco-Ibáñez et al., 1998), and one of the main actions of enkephalin in the hippocampus is disinhibition of principal neurons via modulation of the somatodendritic and axonal compartments of GABAergic interneurons (Zieglgänsberger et al., 1979; Drake et al., 2007).

3.3 Convergence of enkephalinergic and noradrenergic axon terminals in the BLa

Stressful events, including footshock, psychological stress, and fear conditioning, are known to increase norepinephrine (NE) levels in the basolateral amygdala, and other areas of the

brain (Quirarte et al., 1998; Tanaka et al., 2000). The release of NE in the BLa is critical for consolidation of inhibitory avoidance memory, where rats learn to avoid a dark compartment in which they previously were administered footshock (McGaugh 2004). There is evidence that MOR agonists, including ENK, decrease NE release in the BLa, and thereby block NE-mediated memory consolidation (Quirarte et al., 1998; Tanaka et al., 2000). These findings suggest that NE and ENK containing axon terminals in the BLa may be in close proximity to each other, perhaps even contacting the same postsynaptic structures or each other. This would permit released ENK to block NE release by activating MOR receptors in NE terminals via volume transmission.

Indeed, the present study demonstrated that it was common for ENK+ axon terminals to be found within 2–3 μm from NET+ terminals in the 5μm × 5μm fields analyzed in this study. This close proximity should facilitate interactions via volume transmission (Drake et al., 2002). Moreover, approximately 20% of NET+ terminals contacted a structure that also was contacted by an ENK+ terminal, usually a spine or thin distal dendrite, and 6.4% of NET+ terminals were in direct contact with an ENK+ terminal. A common form of synaptic convergence was an ENK+ terminal forming an asymmetrical synapse, and an NET+ terminal forming a symmetrical synapse or apposition, with a spine. This arrangement might permit ENK to modulate presynaptic release of glutamate and NE onto the same spine. In addition, since MORs (Zhang et al., 2013, 2015), β-adrenergic receptors (Farb et al., 2010), and NMDA receptors (Farb et al., 1995) are expressed in spines in the basolateral amygdala there is also the possibility of postsynaptic interactions of ENK, NE, and glutamate that might influence synaptic plasticity (Blair et al., 2001).

4. Experimental Procedures

4. 1. Light microscopy

A total of 10 adult male Sprague-Dawley rats (250–350g; Harlan, Indianapolis, IN) were used in this study. Seven rats were used for light microscopy and three rats were used for electron microscopy. All experiments were carried out in accordance with the National Institutes of Health Guide for the Care and Use of Laboratory Animals and were approved by the Institutional Animal Use and Care Committee (IACUC) of the University of South Carolina. All efforts were made to minimize animal suffering and to use the minimum number of animals necessary to produce reliable scientific data.

Four of the seven rats used for light microscopy were processed for immunoperoxidase histochemistry using DAB (3,3′-diaminobenzidine 4HCl; Sigma Chemical Co., St. Louis, MO, USA) as a chromogen to generate a brown reaction product. These rats were anesthetized with sodium pentobarbital (40 mg/kg, IP) and perfused through the heart with 0.1 M phosphate-buffered saline (PBS; pH 7.4) containing 1% sodium nitrite (100 ml), followed by 4.0% paraformaldehyde and 0.2% picric acid in 0.1 M phosphate buffer (PB; pH 7.4; 500 ml). Following perfusion, brains were removed and postfixed for 3 h in 4.0% paraformaldehyde in PB. Brains were sectioned at 50 μm in the coronal plane using a vibratome. Amygdalar sections were placed in tissue culture chamber slides for immunohistochemical processing. In each brain, a one-in-four series of sections through the amygdala was incubated in a rabbit methionine-enkephalin (ENK) antibody (1:2000; catalog

#20065, RRID: AB_572250, ImmunoStar, Hudson, WI, USA). Adjacent sections were Nissl-stained with cresyl violet. Following an overnight incubation in primary antibody (4 °C), sections were processed for the avidin–biotin immunoperoxidase technique using a rabbit ABC Elite kit (Vector Laboratories, Burlingame, CA, USA) with DAB as a chromogen. All immunoreagents were diluted in PBS containing Triton X-100 (0.3%) and 1% normal goat serum. Following immunohistochemical processing, sections were mounted on gelatinized slides, dried overnight, dehydrated in ethanols, and coverslipped with Permount (Fisher Scientific, Pittsburgh, PA, USA).

Three of the seven rats used for light microscopy were processed for immunoperoxidase histochemistry using nickel-intensified DAB as a chromogen. These rats were anesthetized and perfused through the heart with 0.1 M PBS containing 1% sodium nitrite (100 ml), followed by 4.0% paraformaldehyde in PB (500 ml). They were then processed as described above but with nickel-intensified DAB as a chromogen to generate a black reaction product (Hancock, 1986). In addition, in one of the three brains alternate sections through the entire amygdala were processed for ENK or Nissl stain to enable the plotting of ENK+ neurons in the amygdala using a drawing tube attached to an Olympus BX51 microscope; the Nissl sections were used for determining the boundaries of nuclei in the adjacent ENK-stained sections.

4.2 Electron microscopy

Three rats were anesthetized with an anesthetic mixture (ketamine: 85mg/kg; xylazine: 8mg/kg; acepromazine: 4mg/kg) and perfused intracardially with PBS containing 1% sodium nitrite, followed by 2% paraformaldehyde-3.75% acrolein in PB for 1 minute, followed by 2% paraformaldehyde in PB for 20 minutes. The anesthesia for these rats was switched from the sodium pentobarbital used for the light microscopic studies to the ketamine/xylazine/acepromazine mixture because pharmaceutical grade sodium pentobarbital became unavailable. Brains were removed, postfixed in 2% paraformaldehyde for 1h, and sectioned on a vibratome in the coronal plane at 60μm.

Double-labeling immunohistochemistry was performed to localize ENK, and to analyze the extent of convergence of ENK+ and NET+ terminals onto common structures in the BLa at the ultrastructural level. To enhance penetration of antibodies for the electron microscopic studies, but still preserve ultrastructure, sections were incubated with low levels of Triton X-100 (0.02%) in all of the antibody dilutions. After incubation for 30 minutes in a blocking solution (PBS containing 3% normal goat serum, 1% bovine serum albumin, and 0.02% Triton-X), sections were incubated in a mouse monoclonal NET antibody (1:2000; NET-05; obtained from Dr. Randy D. Blakely, Vanderbilt University Medical Center, Nashville, TN) diluted in blocking solution overnight at 4°C and then processed for the immunoperoxidase technique using a biotinylated goat anti-mouse antibody (1:500; Jackson ImmunoResearch, West Grove, PA, USA) and a Vectastain Standard ABC kit (Vector Laboratories) with DAB as a chromogen. After rinsing, sections were processed with an Avidin/Biotin Blocking Kit (Vector Laboratories). Sections were then incubated overnight at 4°C in the rabbit ENK antibody (1:1000, ImmunoStar) and processed for the immunoperoxidase technique using a biotinylated goat anti-rabbit secondary antibody (1: 500, Jackson ImmunoResearch

Laboratories) and a Vectastain Elite ABC kit with Vector-VIP (Very Intense Purple) as a chromogen (Vector Laboratories). Vector-VIP produces a reaction product that appears purple at the light microscopic level and granular at the electron microscopic level. It was easily distinguished from the diffuse DAB reaction product at the ultrastructural level. Light and electron microscopic examination of sections processed using this dual-labeling immunoperoxidase method, but with one of the two primary antibodies omitted, produced no reaction product for the chromogen associated with the omitted antibody.

After the immunohistochemical reactions, sections were postfixed in 2% osmium tetroxide in 0.16 M sodium cacodylate buffer for 1 h, dehydrated in ethanol and acetone, and flat embedded in Polybed 812 (Polysciences, Warrington, PA) in slide molds between sheets of Aclar (Ted Pella, Redding, CA). Selected areas of the BLa were remounted onto resin blanks. Silver thin sections were collected on formvar-coated slot grids, stained with uranyl acetate and lead citrate and examined with a JEOL-200CX electron microscope. Micrographs were taken with an AMT XR40 digital camera system (Advanced Microscopy Techniques, Danvers, MA).

4.3. Quantitative ultrastructural analysis

The purpose of the quantitative analysis was to study the ultrastructural localization of ENK-ir and to determine the extent to which ENK+ terminals and NET+ terminals converged onto common structures or came into contact with each other. This analysis was modeled after similar studies of the convergence of cortical and dopaminergic inputs to the striatum and basolateral amygdala (Sesack and Pickel, 1990, 1992; Pinto and Sesack, 2008; Pinard et al., 2010). One vibratome section from each of the three rats was selected for thin sectioning and analysis. From these sections, areas that exhibited staining for both ENK and NET were chosen for quantitative analysis. This prerequisite eliminates false negatives due to unequal penetration of reagents (Sesack and Pickel, 1990, 1992). All electron micrographs were taken at 36,000X magnification. For data collection, each NET+ terminal encountered was centered in the field and then ENK+ terminals in the same field were analyzed to determine the extent to which they directly contacted the NET+ terminal or contacted the same structure as the NET+ terminal. Some fields contained two NET+ terminals near the center of the field. The area of each field was 5.0 μm × 5.0 μm. A total of 67 fields containing 78 NET+ terminals and 231 ENK+ terminals were examined. Labeled terminals were followed in 3 to 11 serial thin sections. Contacts of NET+ and ENK+ terminals with ENK-labeled or unlabeled neuronal structures in the BLa were classified as either synapses or appositions. In addition, the types of synapses formed by all ENK+ terminals in these same fields, as well as their postsynaptic targets, were analyzed. Synapses were identified using standard criteria: 1) parallel presynaptic and postsynaptic membranes exhibiting membrane thickening, 2) clustered vesicles associated with the presynaptic membrane, and 3) a synaptic cleft containing dense material. Contacts which did not meet these criteria were identified as appositions. Asymmetrical and symmetrical synapses were identified based on the presence or absence of a prominent postsynaptic density (Peters et al., 1991). Postsynaptic neuronal profiles were identified as ENK+ or ENK-negative somata, large-caliber dendritic shafts (≥1μm), small-caliber dendritic shafts (<1μm), or spines according to established morphological criteria (Peters et al. 1991).

4.4 Antibody specificity

The met-enkephalin antibody (catalog #20065, RRID: AB_572250; ImmunoStar) has very limited recognition of leucine-enkephalin and has no cross reaction with endorphins in immunodot-blot analyses (Cheng et al., 1995). To further characterize the specificity of this antiserum in the amygdala we preadsorbed the antibody (diluted 1:1000) with met-enkephalin (20 μg/ml), dynorphin A (20 and 80 μg/ml), or dynorphin B (20 and 80 μg/ml), and processed the sections for immunoperoxidase histochemistry using nickel-intensified DAB as a chromogen. No staining was seen in the amygdala, or any other brain region, when the antibody was preadsorbed with met-enkephalin, with the exception of a few lightly-stained dendritic processes in the central amygdalar nucleus. No attenuation of ENK staining was seen in any brain region, including the amygdala, when the antibody was preadsorbed with either of the two concentrations of dynorphin A or dynorphin B.

The mouse monoclonal anti-NET primary antibody (1:2000; NET-05, obtained from Dr. Randy D. Blakely, Vanderbilt University Medical Center, Nashville, TN) used in this study was raised against amino acids 5–17 of the amino-terminus of mouse NET. The specificity of this antibody has been demonstrated by absence of staining in NET knock out animals and following preadsorption with the antigenic peptide (Matthies et al., 2009). It has been used to localize noradrenergic terminals in both light and electron microscopic studies (Matthies et al., 2009; Erickson et al., 2011).

Acknowledgments

The authors are grateful for the donation of the monoclonal NET antibody by Dr. Randy Blakely (Vanderbilt University School of Medicine, Nashville, TN). This work was supported by National Institutes of Health Grants R01-DA027305 and R01MH104638.

References

Agnati LF, Fuxe K, Zoli M, Ozini I, Toffano G, Ferraguti F. A correlation analysis of the regional distribution of central enkephalin and beta-endorphin immunoreactive terminals and of opiate receptors in adult and old male rats. Evidence for the existence of two main types of communication in the central nervous system: the volume transmission and the wiring transmission. Acta physiol Scand. 1986; 128:201–207. [PubMed: 3022556]

Asan E. The catecholaminergic innervation of the rat amygdala. Adv Anat Embryol Cell Biol. 1998; 142:1–118. [PubMed: 9586282]

Blair HT, Schafe GE, Bauer EP, Rodrigues SM, LeDoux JE. Synaptic plasticity in the lateral amygdala: a cellular hypothesis of fear conditioning. Learn Mem. 2001; 8:229–242. [PubMed: 11584069]

Blasco-Ibáñez JM1, Martínez-Guijarro FJ, Freund TF. Enkephalin-containing interneurons are specialized to innervate other interneurons in the hippocampal CA1 region of the rat and guinea-pig. Eur J Neurosci. 1998; 10:1784–1795. [PubMed: 9751150]

Brinley-Reed M, Mascagni F, McDonald AJ. Synaptology of prefrontal cortical projections to the basolateral amygdala: an electron microscopic study in the rat. Neurosci Lett. 1995; 202:45–48. [PubMed: 8787827]

Carlsen J, Heimer L. The basolateral amygdaloid complex as a cortical-like structure. Brain Res. 1988; 441:377–380. [PubMed: 2451985]

Cheng PY, Svingos AL, Wang H, Clarke CL, Jenab S, Beczkowska IW, Inturrisi CE, Pickel VM. Ultrastructural immunolabeling shows prominent presynaptic vesicular localization of delta-opioid

receptor within both enkephalin- and nonenkephalin-containing axon terminals in the superficial layers of the rat cervical spinal cord. J.Neurosci. 1995; 15:5976–5988. [PubMed: 7666182]

Drolet G, Dumont EC, Gosselin I, Kinkead R, Laforest S, Trottier JF. Role of endogenous opioid system in the regulation of the stress response. Prog. Neuropsychopharmacol Biol.Psychiatry. 2001; 25:729–741. [PubMed: 11383975]

Drake CT, Chang PC, Harris JA, Milner TA. Neurons with mu opioid receptors interact indirectly with enkephalin-containing neurons in the rat dentate gyrus. Exp Neurol. 2002; 176:254–261. [PubMed: 12093103]

Drake CT, Chavkin C, Milner TA. Opioid systems in the dentate gyrus. Prog Brain Res. 2007; 163:245–263. 2007. [PubMed: 17765723]

Erickson SL, Gandhi AR, Asafu-Adjei JK, Sampson AR, Miner L, Blakely RD, Sesack SR. Chronic desipramine treatment alters tyrosine hydroxylase but not norepinephrine transporter immunoreactivity in norepinephrine axons in the rat prefrontal cortex. Int J Neuropsychopharmacol. 2011; 14:1219–1232. [PubMed: 21208501]

Faber ES, Sah P. Opioids inhibit lateral amygdala pyramidal neurons by enhancing a dendritic potassium current. J. Neurosci. 2004; 24:3031–3039. [PubMed: 15044542]

Farb CR, Aoki C, Ledoux JE. Differential localization of NMDA and AMPA receptor subunits in the lateral and basal nuclei of the amygdala: a light and electron microscopic study. J. Comp Neurol. 1995; 362:86–108. [PubMed: 8576430]

Farb CR, Ledoux JE. Afferents from rat temporal cortex synapse on lateral amygdala neurons that express NMDA and AMPA receptors. Synapse. 1999; 33:218–229. [PubMed: 10420169]

Farb CR, Chang W, Ledoux JE. Ultrastructural characterization of noradrenergic axons and Beta-adrenergic receptors in the lateral nucleus of the amygdala. Front Behav Neurosci. 2010; 4:162. [PubMed: 21048893]

Ferry B, McGaugh JL. Clenbuterol administration into the basolateral amygdala post-training enhances retention in an inhibitory avoidance task. Neurobiol Learn Mem. 1999; 72:8–12. [PubMed: 10371711]

Ferry B, McGaugh JL. Involvement of basolateral amygdala alpha2-adrenoceptors in modulating consolidation of inhibitory avoidance memory. Learn Mem. 2008; 15:238–243. [PubMed: 18391184]

Finley JC, Maderdrut JL, Petrusz P. The immunocytochemical localization of enkephalin in the central nervous system of the rat. J Comp Neurol. 1981; 198:541–565. [PubMed: 7019273]

Finnegan TF, Chen SR, Pan HL. Mu opioid receptor activation inhibits GABAergic inputs to basolateral amygdala neurons through Kv1.1/1.2 channels. J Neurophysiol. 2006; 95:2032–2041. [PubMed: 16306173]

Glass MJ, Kruzich PJ, Colago EE, Kreek MJ, Pickel VM. Increased AMPA GluR1 receptor subunit labeling on the plasma membrane of dendrites in the basolateral amygdala of rats self-administering morphine. Synapse. 2005; 58:1–12. [PubMed: 16037950]

Gray TS, Cassell MD, Kiss JZ. Distribution of pro-opiomelanocortin-derived peptides and enkephalins in the rat central nucleus of the amygdala. Brain Res. 1984; 306:354–358. [PubMed: 6087978]

Galvez R, Mesches MH, McGaugh JL. Norepinephrine release in the amygdala in response to footshock stimulation. Neurobiol Learn Mem. 1996; 66:253–257. [PubMed: 8946419]

Hancock MB. Two-color immunoperoxidase staining: visualization of anatomic relationships between immunoreactive neural elements. Am J Anat. 1986; 175:343–352. [PubMed: 2422916]

Harlan RE, Shivers BD, Romano GJ, Howells RD, Pfaff DW. Localization of preproenkephalin mRNA in the rat brain and spinal cord by in situ hybridization. J. Comp. Neurol. 1987; 258:159–184. [PubMed: 3584538]

Helmstetter FJ, Bellgowan PS, Poore LH. Microinfusion of mu but not delta or kappa opioid agonists into the basolateral amygdala results in inhibition of the tail flick reflex in pentobarbital-anesthetized rats. J Pharmacol Exp Ther. 1995; 275:381–388. [PubMed: 7562575]

Helmstetter FJ, Tershner SA, Poore LH, Bellgowan PS. Antinociception following opioid stimulation of the basolateral amygdala is expressed through the periaqueductal gray and rostral ventromedial medulla. Brain Res. 1998; 779:104–118. [PubMed: 9473612]

Introini-Collison IB, Nagahara AH, McGaugh JL. Memory enhancement with intra-amygdala post-training naloxone is blocked by concurrent administration of propranolol. Brain Res. 1989; 476:94–101. [PubMed: 2914216]

Introini-Collison IB, Ford L, McGaugh JL. Memory impairment induced by intraamygdala beta-endorphin is mediated by noradrenergic influences. Neurobiol Learn Mem. 1995; 63:200–205. [PubMed: 7663894]

Izquierdo I, Graudenz M. Memory facilitation by naloxone is due to release of dopaminergic and beta-adrenergic systems from tonic inhibition. Psychopharmacology. 1980; 67:265–268. [PubMed: 6247739]

Khachaturian H, Lewis ME, Hollt V, Watson SJ. Telencephalic enkephalinergic systems in the rat brain. J Neurosci. 1983; 3:844–855. [PubMed: 6834107]

LeDoux JE, Farb CR, Milner TA. Ultrastructure and synaptic associations of auditory thalamo-amygdala projections in the rat. Exp Brain Res. 1991; 85:577–586. [PubMed: 1717305]

Li R, Nishijo H, Ono T, Ohtani Y, Ohtani O. Synapses on GABAergic neurons in the basolateral nucleus of the rat amygdala: double-labeling immunoelectron microscopy. Synapse. 2002; 43:42–50. [PubMed: 11746732]

Li R, Nishijo H, Wang Q, Uwano T, Tamura R, Ohtani O, Ono T. Light and electron microscopic study of cholinergic and noradrenergic elements in the basolateral nucleus of the rat amygdala: evidence for interactions between the two systems. J. Comp. Neurol. 2001; 439:411–425. [PubMed: 11596063]

Mansour A, Khachaturian H, Lewis ME, Akil H, Watson SJ. Autoradiographic differentiation of mu, delta, and kappa opioid receptors in the rat forebrain and midbrain. J Neurosci. 1987; 7:2445–2464. [PubMed: 3039080]

Mansour A, Hoversten MT, Taylor LP, Watson SJ, Akil H. The cloned mu, delta and kappa receptors and their endogenous ligands: evidence for two opioid peptide recognition cores. Brain Res. 1995; 700:89–98. [PubMed: 8624732]

Marowsky A, Yanagawa Y, Obata K, Vogt KE. A specialized subclass of interneurons mediates dopaminergic facilitation of amygdala function. Neuron. 2005; 48:1025–1037. [PubMed: 16364905]

Mascagni F, McDonald AJ. Immunohistochemical characterization of cholecystokinin containing neurons in the rat basolateral amygdala. Brain Res. 2003; 976:171–184. [PubMed: 12763251]

Matthies HJ, Han Q, Shields A, Wright J, Moore JL, Winder DG, Galli A, Blakely RD. Subcellular localization of the antidepressant-sensitive norepinephrine transporter. BMC neuroscience. 2009; 10:65. [PubMed: 19545450]

McDonald AJ, Pearson JC. Coexistence of GABA and peptide immunoreactivity in non-pyramidal neurons of the basolateral amygdala. Neurosci Lett. 1989; 100:53–58. [PubMed: 2569703]

McDonald AJ, Mascagni F. Colocalization of calcium-binding proteins and GABA in neurons of the rat basolateral amygdala. Neuroscience. 2001; 105:681–693. [PubMed: 11516833]

McDonald AJ, Muller JF, Mascagni F. GABAergic innervation of alpha type II calcium/calmodulin-dependent protein kinase immunoreactive pyramidal neurons in the rat basolateral amygdala. J Comp Neurol. 2002. 2002 May 6; 446(3):199–218.

McDonald AJ, Mascagni F, Mania I, Rainnie DG. Evidence for a perisomatic innervation of parvalbumin-containing interneurons by individual pyramidal cells in the basolateral amygdala. Brain Res. 2005; 1035:32–40. [PubMed: 15713274]

McGaugh JL. The amygdala modulates the consolidation of memories of emotionally arousing experiences. Annu Rev Neurosci. 2004; 27:1–28. [PubMed: 15217324]

Merchenthaler I, Maderdrut JL, Altschuler RA, Petrusz P. Immunocytochemical localization of proenkephalin-derived peptides in the central nervous system of the rat. Neuroscience. 1986; 17:325–48. [PubMed: 3517687]

Muller JF, Mascagni F, McDonald AJ. Synaptic connections of distinct interneuronal subpopulations in the rat basolateral amygdalar nucleus. J Comp Neurol. 2003; 456:217–236. [PubMed: 12528187]

Muller JF, Mascagni F, McDonald AJ. Pyramidal cells of the rat basolateral amygdala: synaptology and innervation by parvalbumin-immunoreactive interneurons. J Comp Neurol. 2006; 494:635–650. [PubMed: 16374802]

Muller JF, Mascagni F, McDonald AJ. Postsynaptic targets of somatostatin-containing interneurons in the rat basolateral amygdala. J Comp Neurol. 2007; 500:513–529. [PubMed: 17120289]

Pape HC, Pare´ D. Plastic synaptic networks of the amygdala for the acquisition, expression, and extinction of conditioned fear. Physiol Rev. 2010; 90:419–463. [PubMed: 20393190]

Paxinos, G.; Watson, C. The Rat Brain in Stereotaxic Coordinates. New York: Academic Press; 1997.

Peters, A.; Palay, SL.; Webster, HD. The Fine Structure of the Nervous System. New York: Oxford University Press; 1991.

Pinard CR, Mascagni F, Muller JF, McDonald AJ. Limited convergence of rhinal cortical and dopaminergic inputs in the rat basolateral amygdala: an ultrastructural analysis. Brain Res. 2010; 1332:48–56. [PubMed: 20346351]

Pinto A, Sesack SR. Ultrastructural analysis of prefrontal cortical inputs to the rat amygdala: spatial relationships to presumed dopamine axons and D1 and D2 receptors. Brain Struct Funct. 2008; 213:159–175. [PubMed: 18340460]

Pitkänen A, Savander M, Nurminen N, Ylinen A. Intrinsic synaptic circuitry of the amygdala. Ann N Y Acad Sci. 2003; 985:34–49. [PubMed: 12724146]

Poulin JF, Castonguay-Lebel Z, Laforest S, Drolet G. Enkephalin co-expression with classic neurotransmitters in the amygdaloid complex of the rat. J Comp Neurol. 2008; 506:943–959. [PubMed: 18085591]

Quirarte GL, Galvez R, Roozendaal B, McGaugh JL. Norepinephrine release in the amygdala in response to footshock and opioid peptidergic drugs. Brain Res. 1998; 808:134–140. [PubMed: 9767150]

Roozendaal B, McEwen BS, Chattarji S. Stress, memory and the amygdala. Nature reviews Neuroscience. 2009; 10:423–433. [PubMed: 19469026]

Sah P, Faber ES, Lopez De Armentia M, Power J. The amygdaloid complex: anatomy and physiology. Physiol Rev. 2003; 83:803–834. [PubMed: 12843409]

Sesack SR, Pickel VM. In the rat medial nucleus accumbens, hippocampal and catecholaminergic terminals converge on spiny neurons and are in apposition to each other. Brain Res. 1990; 527:266–279. [PubMed: 1701338]

Sesack SR, Pickel VM. Prefrontal cortical efferents in the rat synapse on unlabeled neuronal targets of catecholamine terminals in the nucleus accumbens septi and on dopamine neurons in the ventral tegmental area. J Comp Neurol. 1992; 320:145–160. [PubMed: 1377716]

Smith Y, Pare´ D. Intra-amygdaloid projections of the lateral nucleus in the cat: PHA-L anterograde labeling combined with postembedding GABA and glutamate immunocytochemistry. J Comp Neurol. 1994; 342:232–248. [PubMed: 7911130]

Smith Y, Pare´ J-F, Pare´ D. Differential innervation of parvalbumin immunoreactive interneurons of the basolateral amygdaloid complex by cortical and intrinsic inputs. J Comp Neurol. 2000; 416:496–508. [PubMed: 10660880]

Sugita S, North RA. Opioid actions on neurons of rat lateral amygdala in vitro. Brain Res. 1993b; 612:151–155. [PubMed: 8101129]

Tanaka M, Yoshida M, Emoto H, Ishii H. Noradrenaline systems in the hypothalamus, amygdala and locus coeruleus are involved in the provocation of anxiety: basic studies. Eur J Pharmacol. 2000; 405:397–406. [PubMed: 11033344]

Van Bockstaele EJ, Chan J, Biswas A. Ultrastructural evidence for convergence of enkephalin and adrenaline-containing axon terminals on common targets and their presynaptic associations in the rat nucleus locus coeruleus. Brain Res. 1996; 718:61–75. [PubMed: 8925305]

van den Pol AN. Neuropeptide transmission in brain circuits. Neuron. 2012; 76:98–115. [PubMed: 23040809]

Wagner JJ, Caudle RM, Neumaier JF, Chavkin C. Stimulation of endogenous opioid release displaces mu receptor binding in rat hippocampus. Neuroscience. 1990; 37:45–53. [PubMed: 1978741]

Wagner, JJ.; Chavkin, CI. Neuropharmacology of endogenous opioid peptides. In: Bloom, FE.; Kupfer, DJ., editors. Psychopharmacology: the Fourth Generation of Progress. New York: Raven Press; 1995. p. 519-529.

Wilson MA, Mascagni F, McDonald AJ. Sex differences in delta opioid receptor immunoreactivity in rat medial amygdala. Neurosci Lett. 2002; 328:160–164. [PubMed: 12133579]

Woodruff AR, Sah P. Inhibition and synchronization of basal amygdala principal neuron spiking by parvalbumin-positive interneurons. J Neurophysiol. 2007; 98:2956–2961. [PubMed: 17715201]

Zieglgänsberger W, French ED, Siggins GR, Bloom FE. Opioid peptides may excite hippocampal pyramidal neurons by inhibiting adjacent inhibitory interneurons. science. 1979; 205:415–417. [PubMed: 451610]

Zhang J, Muller JF, McDonald AJ. Noradrenergic innervation of pyramidal cells in the rat basolateral amygdala. Neuroscience. 2013; 228:395–408. [PubMed: 23103792]

Zhang J, Muller JF, McDonald AJ. Mu opioid receptor localization in the basolateral amygdala: an ultrastructural analysis. Neuroscience. 2015; 303:352–363. [PubMed: 26164501]

Highlights

- Enkephalin (ENK) is contained in perikarya of interneurons in basolateral amygdala
- Lighter levels of ENK are found in pyramidal neurons in the basolateral amygdala
- ENK is also contained in axon terminals forming excitatory or inhibitory synapses
- ENK terminals and noradrenergic (NA) terminals are often in close proximity
- 20% of NA terminals contact dendrites that are also contacted by ENK terminals

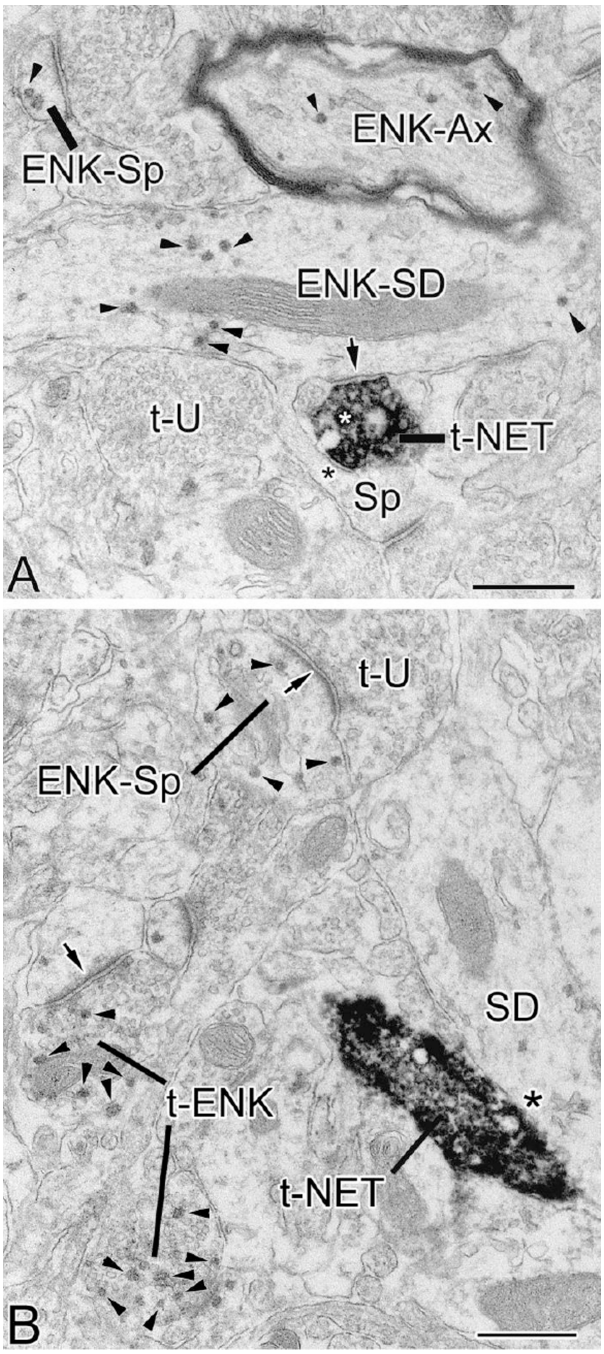

Fig. 1.

Photomicrographs of ENK-ir in the BLC in sections stained with nickel-intensified DAB. (A) ENK-ir at the bregma −2.2 level. Note strong ENK-ir in the central nucleus (including its lateral capsular subdivision [CLC]) and caudate-putamen (CP), and moderate ENK-ir in the intercalated nuclei located in the external capsule along the lateral (left) border of the anterior subdivision of the basolateral nucleus (BLa). The BLa and dorsolateral subdivision of the lateral nucleus (Ldl) have light neuropilar ENK-ir and scattered nonpyramidal neurons that exhibit intense ENK-ir (see C for a view of the BLa at higher magnification). (B) ENK-

ir at the bregma −3.0 level. Note strong ENK-ir in the central nucleus (including its lateral subdivision [CL]), caudate-putamen (CP), and intercalated nuclei (including one located at the border of the lateral and basolateral nuclei [IN]). All nuclei of the BLC, including the dorsolateral, ventromedial and ventrolateral subdivisions of the lateral nucleus (Ldl, Lvm, Lvl), the anterior, posterior and ventral subdivisions of the basolateral nucleus (BLa, BLp, BLv), and the anterior basomedial nucleus (BMa) have light neuropilar ENK-ir and scattered nonpyramidal neurons that exhibit intense ENK-ir (see D and Fig. 2A for higher power views of the BLa at this level). The stronger neuropilar staining of the lateral nucleus versus the other nuclei of the BLC is due to a higher density of ENK+ axons in this nucleus (see Fig. 2B). (C and D) Higher power photomicrographs of the ventral parts of BLa shown in A and B, respectively (asterisks mark the same blood vessels in A/C and B/D). Note intense ENK-ir in small nonpyramidal neurons (arrows show three representative examples in each pane). In addition, there are numerous larger putative pyramidal neurons with light ENK-ir in the ventral part of BLa (C; above the blood vessel marked with an asterisk) and ventromedial corner of BLa (D; below and to the right of the blood vessel marked with an asterisk) (arrowheads show four representative examples in each pane). Scale bars = 200 μm in A (B is at the same magnification), 100 μm in C (D is at the same magnification).

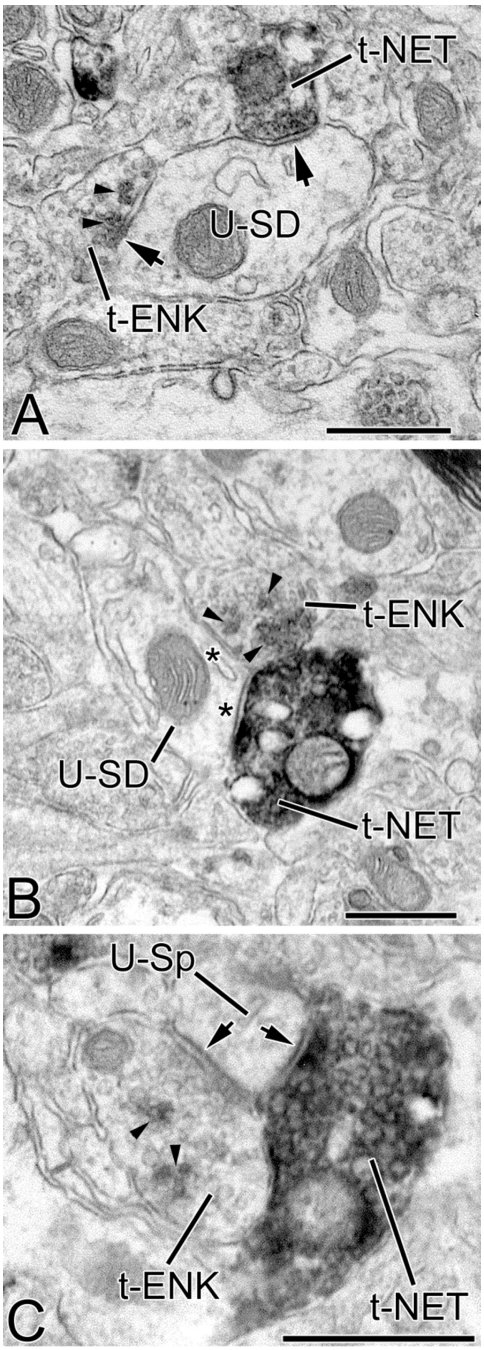

Fig. 2.

(A) High power photomicrograph of ENK-ir in the BLa in a section stained with nickel-intensified DAB. This field contains two ENK+ nonpyramidal neurons that are in the plane of focus, and numerous small ENK+ puncta presumed to be axon terminals; an axon with large varicosities (1 μm in diameter) is indicated with an arrow. (B) High power photomicrograph of ENK-ir in the lateral nucleus in a section stained with nickel-intensified DAB. This field contains numerous ENK+ puncta that average about 1 μm in diameter and appear to be axon terminals. (C) Four small ENK+ nonpyramidal neurons in the BLa in a

section stained with non-intensified DAB. Small ENK+ puncta can be seen in the neuropil. (D) NET+ axons in the BLa. All scale bars = 25μm.

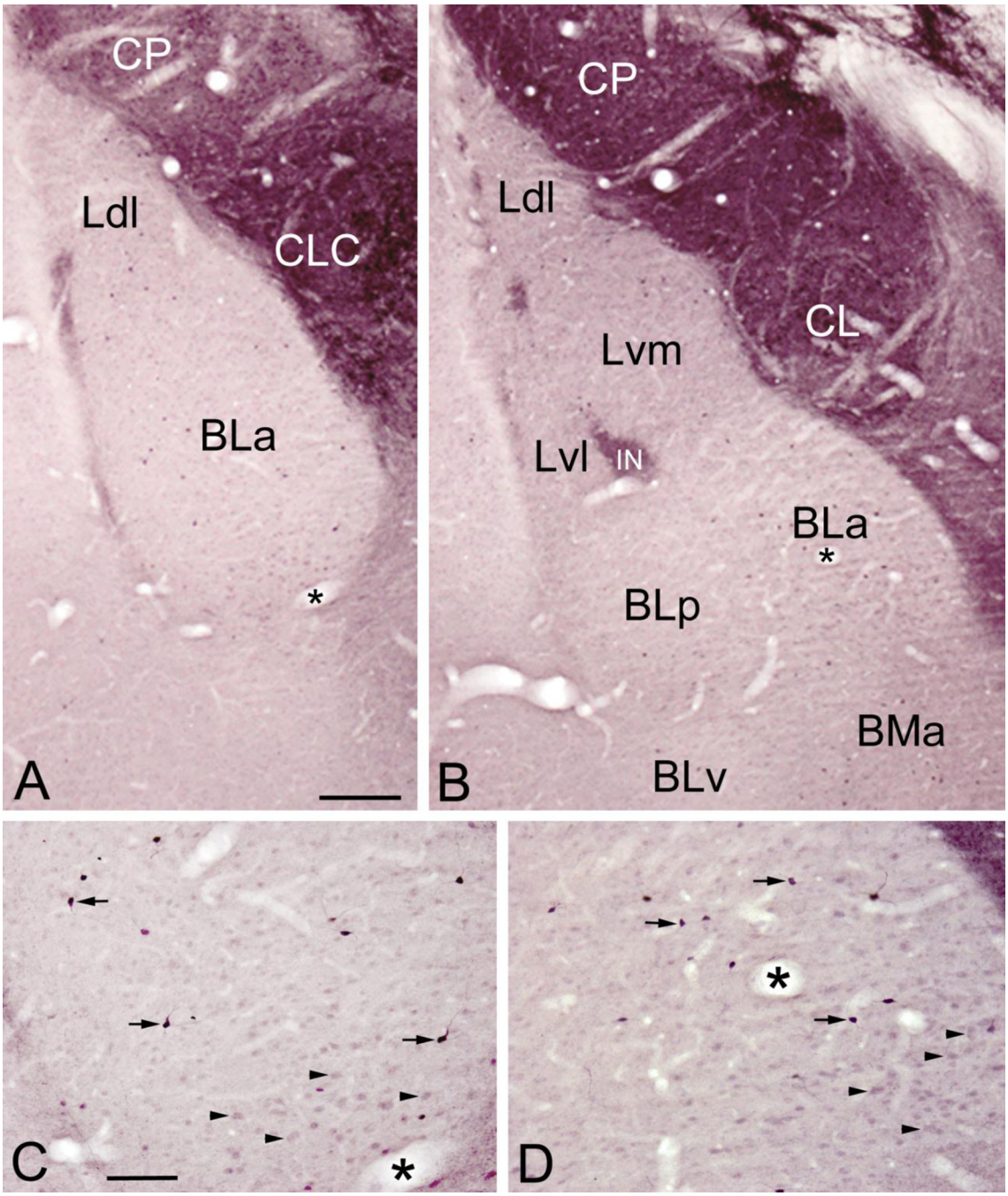

Fig. 3.

Plots of ENK+ nonpyramidal neurons in the BLC and cortical nuclei at rostral (A), middle (B) and caudal (C) levels of the amygdala. Drawings of brain sections are from the atlas by Paxinos and Watson (1997). Neurons are plotted from two non-adjacent sections at each level. Each dot represents one neuron. The central nucleus and intercalated nuclei contained a much higher density of neurons, but these are not plotted. Abbreviations: ACo, anterior cortical nucleus; AHA, amygdalohippocampal area; AStr, amygdalostriatal transition area; BLa, anterior basolateral nucleus; BLp, posterior basolateral nucleus; BLv, ventral

basolateral nucleus; BMa, anterior basomedial nucleus; BMp, posterior basomedial nucleus; CL, lateral central nucleus; CeC, capsular central nucleus; CM, medial central nucleus; CP, caudate-putamen; IN, intercalated nucleus; Ldl, dorsolateral lateral nucleus; Lvm, ventromedial lateral nucleus; Lvl, ventrolateral lateral nucleus; Mad, anterodorsal medial nucleus; Mav, anteroventral medial nucleus; Mpd, posterodorsal medial nucleus; Mpv, posteroventral medial nucleus; OT, optic tract; PC, piriform cortex; PLCo, posterolateral cortical nucleus; PMCo, posteromedial cortical nucleus; ST, stria terminalis; VEn, ventral endopiriform nucleus.

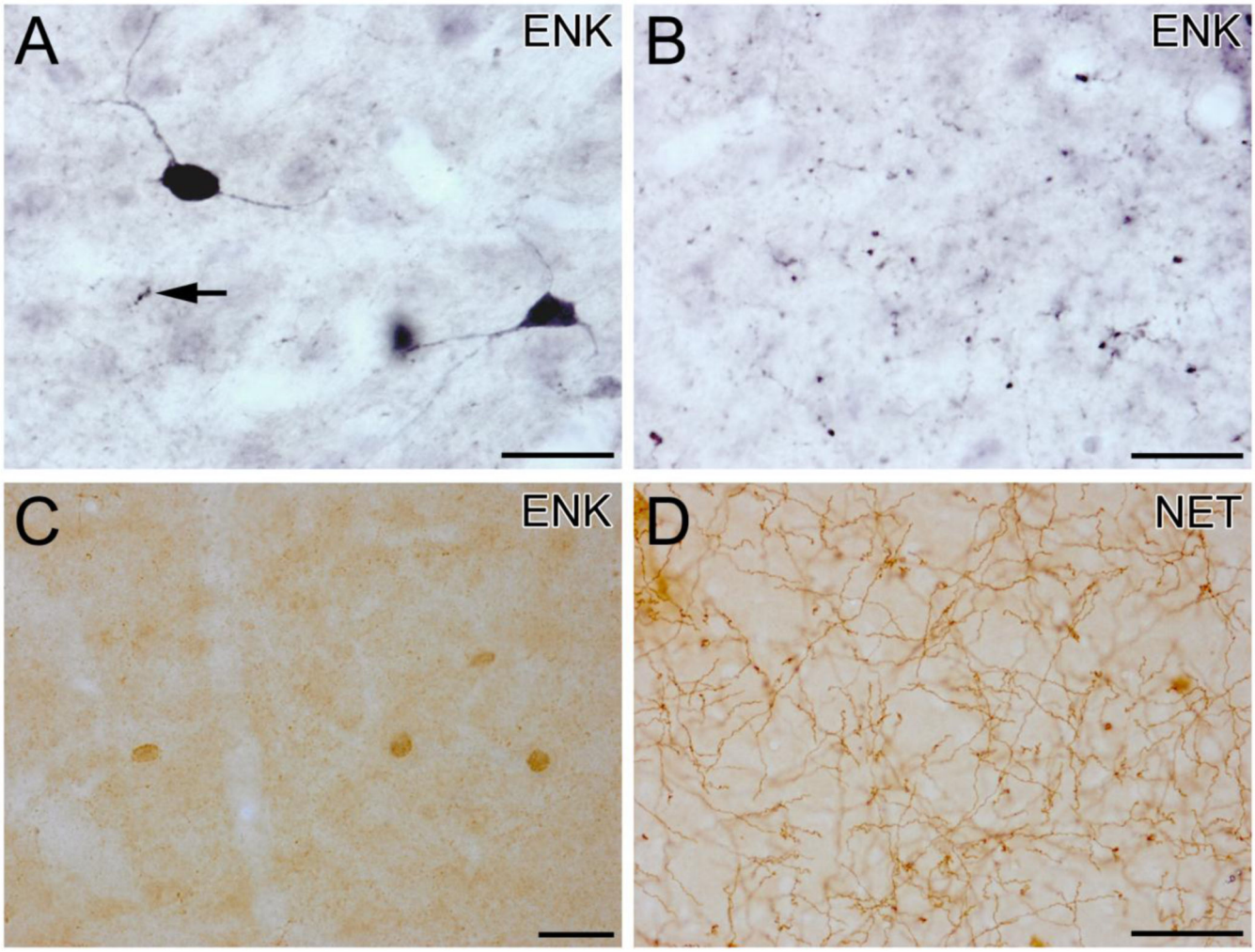

Fig. 4.

Electron micrographs of ENK-ir (particulate Vector-VIP reaction product) and NET-ir (dense, diffuse DAB reaction product) in the BLa. Small arrowheads indicate representative Vector-VIP particles in ENK+ structures. (A) In this field ENK-ir is found in various structures including a myelinated axon (ENK-Ax), spine head (ENK-Sp), and a small-caliber dendrite (ENK-SD) that gives rise to an unlabeled spine (Sp); an NET+ axon terminal (t-NET) containing a large dense core vesicle (white asterisk) contacts both this dendrite as well as its spine. The former contact appears to be a symmetrical synapse (arrow) while the latter was judged to be an apposition (black asterisk). An unlabeled terminal (t-U) is also in the field. (B) An NET+ axon terminal (t-NET) forms an apposition (asterisk) with a small-caliber dendrite (SD) that is very lightly labeled for ENK. This field also contains an unlabeled axon terminal (t-U) that forms an asymmetrical synapse (arrow) with an ENK+ spine (ENK-Sp). Two ENK+ axon terminals are seen in the lower right corner (t-ENK); the upper terminal forms an asymmetrical synapse (arrow) with an unlabeled spine. Scale bars = 0.5 μm.

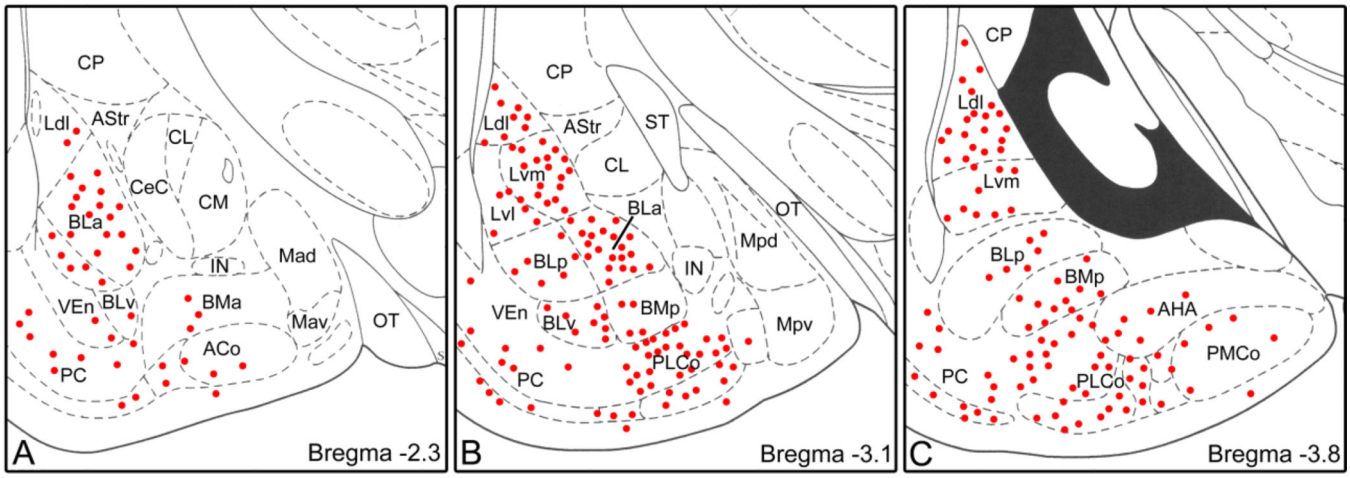

Fig. 5.

Electron micrographs showing convergence of ENK+ (t-ENK) and NET+ terminals (t-NET) onto unlabeled small-caliber dendritic shafts (U-SD in A and B) and an unlabeled spine (U-Sp in C) in the BLa. Small arrowheads indicate representative Vector-VIP particles in ENK+ structures. In A the contacts of both terminals were symmetrical synapses (arrows). The synaptic nature of the ENK+ terminal was more evident in other sections of the series. The NET+ terminal is #EM08-T29 of Table 2. In B the ENK+ terminal and the NET+ terminal form appositions (asterisks), and are also apposed to each other. The NET+ terminal is #EM11-T07 of Table 2. In C the ENK+ terminal and the NET+ terminal both form symmetrical synapses and are in contact with each other. The NET+ terminal is #EM11-T42 of Table 2. Scale bars = 0.5 μm.

Table 1

Postsynaptic targets of ENK+ axon terminals forming asymmetrical (AS) or symmetrical (S) synapses in the BLa. No somata were postsynaptic to ENK+ terminals in the quantitative survey. ENK-positive and ENK-negative structures are indicated with a plus sign (+) or a minus sign (−), respectively. Abbreviations: LD, large-caliber dendrite (>1.0 μm wide); SD, small-caliber dendrite (<1.0 μm wide); Sp; spine.

Synapse Type	LD+	LD−	SD+	SD−	Sp+	Sp−	Total
AS	1 (0.7%)	0 (0.0%)	11 (7.8%)	2 (1.4%)	92 (64.5%)	36 (25.6%)	142 (100%)
S	9 (36.0%)	0 (0.0%)	14 (56.0%)	1 (4.0%)	0 (0.0%)	1 (4.0%)	25 (100%)

Table 2

Targets and types of contacts of converging ENK+ terminals and NET+ terminals in the BLa. Contacts were asymmetrical synapses (AS), symmetrical synapses (S), or appositions (non -synaptic contacts). ENK-positive and ENK-negative structures are indicated with a plus sign (+) or a minus sign (−), respectively.
Abbreviations: So: soma; LD: large-caliber dendrite (≥1μm); SD: small-caliber dendrite (<1μm); Sp: spine.

NET+ Terminals	Target	ENK Contact	NET Contact
EM08-T2	Sp+	AS	S
EM08-T24	Sp+	AS	Apposition
EM11-T50	Sp+	AS	Apposition
EM08-T16	Sp−	AS	Apposition
EM08-T19	Sp−	AS	S
EM11-T42	Sp−	S	S
EM08-T21	SD+	AS	S
EM08-T22	SD+	S	S
EM08-T31	SD+	Apposition	Apposition
EM08-T29	SD−	S	S
EM10-T13	SD−	AS	Apposition
EM11-T04	SD−	S	Apposition
EM11-T05	SD−	Apposition	S
EM11-T07	SD−	Apposition	Apposition
EM10-T07	LD+	Apposition	Apposition
EM10-T25	So+[1]	Apposition	S

[1] ENK-ir in this So+ soma was confined to the Golgi complex